Antibacterial activity of In-doped ZnO nanoparticles

Enas N. Danial[1,2], M. Hjiri[3,4], M. Sh. Abdel-Wahab[5,6], N.H. Alonizan[7,8], L. El Mir [4] and M.S. Aida[3,5]*

[1] Biochemistry Department, Faculty of Sciences Jeddah University, Jeddah, Saudi Arabia.
[2] Department of Chemistry of Natural and Microbial Products, National Research Center, Dokki, Cairo, Egypt
[3] King Abdulaziz University, Faculty of Sciences, Department of Physics, Jeddah, Saudi Arabia.
[4] Laboratory of Physics of Materials and Nanomaterials Applied at Environment, Faculty of Sciences of Gabes, 6072 Gabes, University of Gabes, Tunisia
[5] Center of Nanotechnology, King Abdulaziz University, Jeddah, Saudi Arabia

[6] Materials Science and Nanotechnology Department, Faculty of Postgraduate Studies for Advanced Sciences, Beni-Suef University, Beni-Suef, Egypt

[7] Department of Physics, College of Science, Imam Abdulrahman Bin Faisal University, P.O. Box 1982,31441 Dammam, Saudi Arabia

[8] Basic and Applied Scientific Research Center, Imam Abdulrahman Bin Faisal University, P.O. Box 1982,31441 Dammam, Saudi Arabia

* Corresponding authors (M.S. Aida) e-mail: aida_salah2@yahoo.fr

Abstract

In the present work, undoped and In-doped zinc oxide (ZnO) nanoparticles have been prepared by sol gel technique. Different In dopant concentration ranged from 1 to 5 at. % has been used. The structural and morphological properties of the obtained nanoparticles have been studied using respectively X-ray diffraction (XRD), Raman spectroscopy and scanning electron microscopy (SEM). The electronic defects in the nanopowder band gap were investigated by photoluminescence (PL) spectroscopy. The antibacterial activities of the prepared nanopowders have been tested against Gram positive and Gram negative bacteria's. Based on the inhibition zone determination, the results indicated that In dopant improves its antibacterial activity. The In doping effect is explained in term of the electronic defect enhancement such as inertial defect Z_{ni} and vacancy defect V_{zn} with In doping, these two defects act as source of electrons and holes during the reactive oxygen species (ROS) production responsible for bacteria's destruction. Due to the bonded hydrogen charge transfer crystal screening, the prepared ZnO nanoparticles exhibit a low antioxidant activity.

Keywords: *Nanoparticle; ZnO; Antibacterial activity; Sol- gel*

1. Introduction

Zinc oxide has attracted an increasing interest due to its excellent semiconducting properties. ZnO is a direct wide band gap of 3.37 eV, it enjoys a large excitation binding energy (60 meV) at room temperature and thermal stabilities [1–3]. ZnO is becoming the most used semiconducting metallic oxide; it has received a considerable attention as a promising material in a wide range of technological applications namely: electronics, optics and optoelectronics devices transparent conducting oxide (TCO), gas sensing, waste water treatment, nanogenerator, and antibacterial activity.

Nowadays microbial contamination is becoming a serious issue in healthcare and food industry. Annually 40 % of the 50 million deaths in world were due to infectious diseases caused by bacteria's such as Escherichia coli, Salmonella etc... [4-6].

Therefore, developments of nanoparticles with antimicrobial properties are of considerable interest. In the last few years, multi-functional metals and metal oxides have attracted interest for their antimicrobial activities [7]. Metal oxide nanoparticles find many applications in physical, chemical and biological fields, including bio labeling and antibacterial agents [8]. Metal oxides nanoparticles, such as TiO_2 [9], ZnO [10], CuO [11], SiO_2 [12], SnO_2 [13] and MgO [14]] have shown significant antibacterial properties. Among these metal oxides nanomaterials, ZnO is of special interest due to its established use in health care products, UV blocking biocompatibility. The antibacterial activity of ZnO NPs was reported earlier [15, 16]. It has been demonstrated that ZnO nanostructures can effectively be used both against Gram-positive and Gram-Negative bacteria [17, 18].

The antibacterial action of a material mainly depends on the production of reactive oxygen species on the surface of the nanoparticles. The mechanisms of actions are proposed such as generation of reactive oxygen species (ROS) or release of Zn^{2+} ions. Both of them lead to harmful interaction with cell membranes of bacteria and cause cell death [19].

It is well established in literature that impurity doping into ZnO host matrix can tune various properties of ZnO and enhance its antibacterial activity [20-22]. Several doping elements effect on ZnO antibacterial activity have been investigated in the literature. The antibacterial activity of Co doped ZnO [23] , Fe doped ZnO [24,25], Ni doped ZnO [26,27], V doped ZnO [28], Sn doped

ZnO [29] , Ag doped ZnO [30] , Mg doping [31,32], Mn doped ZnO [33,34], Sr doped ZnO [35], Sc doped ZnO [36], Se doped ZnO [37]. Also co-doping with F and Fe [38], La and Cu co-doped ZnO [39] have been also investigated. To the best of our knowledge in doping effect on ZnO nanopowder antibacterial activity has not been investigated. The only complied work is that reported by Manoharan et al [40] in doped thin film prepared by spray pyrolysis.

In the present study we investigated the antibacterial activity of In-doped ZnO nanopowders prepared via sol-gel technique. The antibacterial activity of the prepared nanopowders are tested against various Gram positive (*Bacillus subtilits, Staphylococcus aureus*) and Gram negative (*Escherichia coli, Pseudomonas aeruginosa*) bacteria's.

2. Experimental details

2.1. Samples synthesis

The sol-gel technique is used to prepare undoped and In-doped ZnO nanoparticles with different In doping ratio (0, 1, 3 and 5 at.%) by dissolving 16 g of zinc acetate dehydrate Zn(CH3COO)2.2H2O; 99% as precursor in a 112 ml of methanol. After magnetic stirring at room temperature for 10 min, an adequate quantity of indium chloride ($InCl_3$) corresponding to a ratio [In]/[Zn] of 0.01, 0.03, 0.05 was added . After 15 min magnetic stirring, the solution was poured in an autoclave and dried under ethyl alcohol (EtOH) at supercritical conditions. The obtained nanopowders were then heat treated at 400 °C for 2 hours in air in an open oven.

2.2. Samples Characterization

X-ray diffraction patterns were recorded in the 2θ range from 20° to 80° using a Bruker diffractometer with a Ni β-filtered Cu-Kα radiation. The nanopowder structure was also analyzed by Raman spectroscopy by mean of Lab RAM HR evolution Raman spectrometer. SEM images of the samples surface were acquired by Zeiss Cross Beam 540 instrument, equipped by an EDX spectrometer.

The photoluminescence (PL) measurements were carried out by a NanoLog modular spectrofluorometer Horiba with a Xe lamp as the excitation light source at room temperature. An excitation wavelength of 325 nm was applied, and emission was recorded between 350 and 870 nm.

2.3. Biological activity

2.3.1. Tests for antibacterial activity

The accompanying two gram-positive bacteria were utilized: *Bacillus subtilits* NRRL-B-4219, and *Staphylococcus aureus* (ATCC 25923) additionally the gram-negative microorganisms *Escherichia coli*, ATCC 25922 and *Pseudomonas aeruginosa* NRRL B23 27853. The antibacterial tests were completed by the well diffusion method [41] to compere the antibacterial activity of undoped and In-doped ZnO nanoparticles against the human pathogenic bacteria. Neomycin was utilized as guidelines with focus 30µg/ml. The bacterial suspensions were balanced with saline to a convergence of 10^5 CFU/ml. The inoculum was refined on nutrient medium to confirm the nonattendance of tainting and to check the legitimacy of the inoculum. Societies were spread onto the plates, and afterward wells were made by utilizing cork borer (8mm). Wells were stacked with: 10 µg/mL of engineered mixes weakened with dimethyl sulfoxide (DMSO) at focuses (10µg/mL) were added to each well independently. The Petri dishes were kept aseptically for roughly 4 to 5h for dissemination of the example. Following, all the Petri dishes were incubated for 24 h at 32º C, then the development inhibition zones was estimated.

2.3.2. Antioxidant activity DPPH assay

DPPH (1, 1-Diphenyl-2-picrylhydrazyl) assay is one of the most extensively used method for determining the antioxidant potential of any biological sample [42]. DPPH is a purple stable free radical which is reduced to yellow colored complex DPPH-H (1, 1-diphenyl-2-picrylhydrazine) by the compounds which are capable of donating hydrogen or electron. The absorbance of the mixture was read at 517 nm in a spectrophotometer. The decrease in absorbance indicates increase in DPPH free radical scavenging potential. The percentage inhibition was calculated by the following equation.

$$\text{DPPH free radical Scavenging (\%)} = [(\text{Abs control} - \text{Abs sample}) / \text{Abs control}] \times 100$$

Where, Abs control is the absorbance of control and Abs sample is the absorbance of sample. Lower absorbance of the reaction mixture indicates higher free radical scavenging activity.

3. Results and discussion

Figure 1 represents XRD diffraction pattern recorded for the undoped and In-doped ZnO synthetized nanopowder with different doping concentration. The obtained nanopowders are polycrystalline, the pattern of different samples are composed of different peaks assigned to the diffraction plan (100), (002), (102), (110), (103) and (112) of the ZnO Wurtzite hexagonal structure (according to JPCD card No. 36-1451). The pattern do not contain other peaks origination from to a secondary related to In indicating the pure quality of the synthetized nanopowder and also that In is incorporated in the ZnO lattice and do not form any secondary phase such Indium oxide. The direction (101) has a preferential orientation in all powder. The same preferential orientation has been observed in Fe doped ZnO [23, 24], Ni doped ZnO [25], V doped ZnO [28] and in Mg doped [31]. This preferential orientation seem to be an intrinsic properties of ZnO nanopowder. While the ZnO thin films are characterized by the preferential orientation along the direction (002) [43]. This discrepancy can be attributed to the difference in the involved growth mechanism during thin film and nanopowder formation.

The crystallite size is calculated using Hall–Williamson method [44]. The estimated crystallite sizes are reported in Figure 2. As seen, the crystallite size is reduced from 84 nm to 34 nm with increasing the doping ratio. The same drastic effect of In doping on the crystallite size has been also reported in In doped ZnO thin films by Manoharan et al [40]. The reduction of the crystallite size may be due to the increase in the nucleation center with the introduction of In. It is well know that any foreign atom or impurity in the solution acts as a nucleation center for ZnO nanocrystal. The same behavior have reported in Ni doped ZnO [25] and Mg doped ZnO [31] nanoparticles.

Figure 3 shows the Raman spectra recorded in undoped and In-doped ZnO nanopowder. With different levels. The symmetrical peak located at 437 cm^{-1} is assigned to the E_2 (high) originating from the lattice vibration of oxygen atoms [45]. This peak is a characteristic of ZnO phase and reported by several authors in various ZnO nanostructure [46, 47]. As well as deduced from XRD, there is no peak originating from secondary phase indicating the purity of the prepared powder in one hand and to the introduction of In atoms in the host ZnO lattice on the other hand. As can be seen, the peak E_2 increases with In doping, the increase of the intensity of this peak with doping has been also observed in Al doped ZnO [48].

The nanopowder morphology was studied using SEM observation. Figures 4 show the SEM images of undoped and In-doped ZnO nanopowder. The nanopowders are composed of agglomeration of spherical nanoparticles. In undoped ZnO nanopowder the grains have a homogeneous size. However, indium incorporation rends the grain larger with a non-homogeneous size. Increasing the In doping results in increasing the grain size. The incorporation of Li ions into Zn lattice sites alters the nanoparticles morphological, it favors the small particles agglomeration leading to a larger grains. Several authors have reported that ZnO doping with metallic element changes the shape and the size of the ZnO nanoparticles morphology.

Photoluminescence (PL) spectroscopy is a widely used tool for characterizing the electronic defects and the relative position of their associated level in band gap of the semiconductor. ZnO is known to have a large number of native defects such as zinc vacancies (V_{zn}), oxygen vacancies (V_o) , zinc interstitial (Zn_i) and oxygen inertial (O_i). [49]. The PL spectra of undoped and In doped ZnO nanopowder are shown in Figure 5. The undoped ZnO spectrum exhibits two peaks: a low one near band edge (NBE) located in the UV region at 379.6 nm due to band to band transition [50] and a dominant and broad one in the green region centered at 553.6 nm. The later visible emission is assigned to electronic transition from interstitial Zn_i defect towards the oxygen vacancy defect V_o [51].

The introduction of In in ZnO network is accompanied by the PL spectrum modification as seen in figure 5. It well argued that introduction of doping atoms in the semiconductor network is usually accompanied by the creation of defect levels within the material band gap. In doped ZnO spectrum is characterized by the emergence of new emission peaks: a peak centered at 439.6 nm, due to the transition from Zn_i level towards Zinc vacancy. The second new peak is centered at 667.8 nm due to the transition from Zni towards the oxygen interstitial site. From this analysis one can conclude that In incorporation in ZnO yields to the increase in Zni defects, the formation of Zn vacancies, oxygen interstitial and the reduction in oxygen vacancies.

Undoped and In-doped ZnO NPs are tested against two Gram negative (G+) bacteria's (*Bacillus subtilits, Staphylococcus aureus*) and two Gram positive (G-) (*Escherichia coli, Pseudomonas aeruginosa)* using the Muller Hinton agar disc diffusion method to determine their applicability as an antibacterial agent.

The antibacterial activity is estimated from the inhibition zone diameter (ZOI) as shown in Figure 6. In-doped ZnO exhibits a remarkable antibacterial activity. The data represented in figure 7 is the measured inhibition zone diameter in undoped and In doped ZnO nanoparticles against different bacteria's. As can be deduced ZnO doping with In enhances the antibacterial activity resulting in increasing the ZOI from 11 mm in undoped ZnO to 16.9 nm in 3% In doped ZnO. As regrouped in table I , most of antibacterial activity studies comfort that metallic doping of ZnO results in increasing its antibacterial activity against the whole studied bacteria's. This may due to the contribution of the electronic defects induced by the metallic doping as deduced from Pl studies.

According to the reported values in table I, Indium and Vanadium doping leads to better ZnO antibacterial activity, this might be due to larger ionic radius of In and V by comparison to the other studied metals, they are equal to 0.8 nm which are larger than Mn ionic radius (0.7nm), Ni ionic radius (0.7nm), Mg ionic radius (0.65nm), Co ionic radius (0.6 nm). Doping metal with larger radius ionic metal may introduces various electronic defects in ZnO band gap that play a crucial role in the antibacterial mechanism. This may suggest that the electronic defects in ZnO band gap play a crucial role in its antibacterial activity.

Several mechanisms of ZnO action against bacteria have been suggested. These mechanisms are based on the decomposition of ZnO and formation of reactive oxygen species (ROS) [52]. The reactive oxygen species (ROS) are composed of superoxide $\bullet O_2^-$, hydroxyl radical OH• and hydrogen peroxide H_2O_2, these species can cause damage to DNA and cellular proteins and may lead to the cell death and consequently the formation of a zone of inhibition (ZOI) around the nanomaterials.

The ZnO antibacterial activity and potency and thereafter the size of ZOI are strongly influenced by ZnO nanoparticle properties and morphology [31, 32] It is well argued that the antibacterial efficiency depends on the number of generated hydroxyl radicals [53] and crystallite size of the nanoparticle. The ROS species generation is linked to the electron holes pairs. Free electrons produce the superoxide radical $\bullet O^{2-}$ after reaction with O_2 according to the equation :(Eq. (1)):

$$e^- + O_2 \longrightarrow \bullet O_2 \qquad (1)$$

While holes produce the hydroxyl radical OH• according to the following equations (Eq2, Eq3):

$$h^+ + H_2O \longrightarrow OH^- + H^+ \quad (2)$$

$$h^+ + OH^- \longrightarrow OH\bullet \quad (3)$$

Subsequently the hydrogen peroxide H_2O_2 is generated according to the equation below:

$$2\bullet O_2 + 2\,H^+ \longrightarrow H_2O_2 \quad (4)$$

The free charges can be produced by light absorption that generate electrons in the conduction band leaving a hole in ZnO valence band. This mechanism is used in photoctalytic activity of ZnO using the UV illumination [42]. While in dark or under visible light (with photon energy less that the ZnO band gap) which is the situation in the antibacterial activity , electrons and hole sources are the electronic defect such as negatively charged Zni defect that can be a source of electrons and the positively charged Zinc vacancy V_{zn} defect as holes source. As deduced from PL study these two defects increase with In doping. This suggests that Zn_i and V_{zn} defects play an important role in the production of ROS responsible for bacteria inhibition. Figure 8 is a schematic drawn illustrating these two defects contribution in the ROS generation .The increase in the inhibition zone with In doping as shown in Figure 7 is due to the Zni and V_{zn} defects enhancement with In doping level. Moreover, the increase in the ZOI can be attributed also to the decrease in the ZnO crystallite size. Several authors have mentioned that the reduction in the crystallite size boosts the antibacterial activity due to the enhancement of the crystallite surface activity [26, 35, 38]. Therefore, the observed increase in the ZOI with In doping is in good concordance with the reduction in ZnO crystallite size (Figure 2).

An intriguing feature is that the undoped and In doped ZnO exhibit a low antioxidant behavior as can be deduced from the DPPH assay results reported in figure 9 showing a low free radical scavenging percentage. The low antioxidant activity have been also reported in ZnO nanoparticles prepared by green chemistry, by Tetteya et al [54]. Das et al [55] have also reported that DPPH radical scavenging activity is not enough to claim the antioxidant potential ZnO nanoparticles activity using DPPH free radical scavenging assay.

It worth noting that the antioxidant activity is mainly based on the hydrogen bonded charge transfer, according to the proton coupled electron transfer reaction [56], resulting to the transformation of proton H^+ and electron to an organic radical yielding to the change of DPPH radical to a stable DPPH-H complex. [57]. The observed low antioxidant activity might be due to

the hydrogen bonded charge transfer screening [58]. The low antioxidant activity can be also attributed to the large crystallite size of the synthetized nanopowder ranged from 80 to 30 nm (Figure3). Asok et al [57] studied the antioxidant activity in ZnO particle with a size ranged from 50 to 3 nm , they inferred that nanoparticle size play an important role in the antioxidant activity, they concluded that smaller ZnO nanoparticle size exhibit superior antioxidant activity .

4. Conclusion

In the present work, undoped and In-doped ZnO nanoparticles have been successfully synthetized by sol gel route. The In doping ratio has been varied in the range of 1 to 5% in order to investigate its effect on the nanopowder structural properties and their potential application as antibacterial agent. The XRD and Raman analysis reveal that the prepared nanopowder have the Wurtzite nanocrystalline structure, the In doping results in the crystallite size reduction. The PL study indiacted that In doping cause the formation of electronic defect in the ZnO band gap namely Zn interstitial defect (Zni) and Zn vacancy (Vzn). The formation of this defect explain the origin of the improvement of the In doped ZnO antibacterial activity against Gram positive and Gram negative bacteria's, suggesting that 3% In doped ZnO can be a serious candidate as antibacterial agent against several variety of bacteria's. However, a low antioxidant activity of the prepared nanopowder is observed, this is attributed to the bonded hydrogen charge transfer crystal screening and the large size of the prepared nanoparticle crystallites.

References

[1] C. Klingshirn, Phys. Status Solidi B71 (1975) 547.

[2] T. Minami, Mater. Res. Soc. Bull. 25 (2000) 38.

[3] H. Nanto, T. Minami, S. Takata, J. Appl. Phys. 60 (1986) 482.

[4] L.P. Lukhele, B.B. Mamba, M.N. Momba, R.W. Krause, , J. Appl. Sci. 10 (2010) 65.

[5] M.T. Moustafa, Water Sci. 31 (2017) 164.

[6] T.C. Chiu, Int. J.Mol. Sci. 15 (2014) 7266.

[7] N. Beyth, Y. Houri-Haddad, A. Domb, W. Khan and R. Hazan,, Altern. Med. 2015 (2015) 1.

[8] S. Kaviya, J. Santhanalakshmi, B. Viswanathan, J. Muthumary, K. Srinivasan, Spectrochim. Acta Part A 79 (2011) 594.

[9] F. Sayılkana, M. Asilturka, N. Kirazb, E. Burunkayab, E.A rpac, Hikmet Sayılkan ,J. Hazard. Mater. 162 (2009) 1309.

[10] J. Aanchal, B.Richa, P.Pankaj,Mater.Sci.Eng.C. 33 (2013) 1247.

[11] O. Akhavan, E.Ghaderi, Surf.Coat.Technol. 205 (2010) 219.

[12] X. Bingshe, N.Meia, W.Liqiao, H. Wensheng, L.Xuguang,J. Photochem. Photobiol.A.

Chem. 188 (2007) 98–105.

[13] C. Karunakarann, R.S.Sakthi,P. Gomathisankar, Mater. Sci.Semicond. Process.16 (2013) 818.

[14] J. Sawai, T. Yoshikawa,J. Appl. Microbiol. 96 (2004) 803.

[15] R. Brayner, R. Ferrari-Iliou, N. Brivois, S. Djediat, M.F. Benedetti, F. Fievet, Nano

Lett. 6 (2006) 866.

[16] G.X. Tong, F.F. Du, Y. Liang, Q. Hu, R.N. Wu, J.G. Guan, X. Hu, J. Mater. Chem. B 1

(2013) 454.

[17] R.R. Krishna, T.K.Ranjit, C. M.Adhar, Langmuir 27 (2011) 4020.

[18] J. Nicole, R. Binata,T.R.Koodali,C.M.Adhar, Microbiol.Lett. 279 (2008) 71.

[19] K. Vijayalakshmi, D. Sivaraj, RSC Adv. 5 (2015) 68461

[20] R. Yousefi, F. Jamali-Sheini, M. Cheraghizade, S.Khosravi-Gandomani, A. Saıaedi, N. M. Huang, W.J. Basirun, M.Azarang, Mater. Sci. Semicond. Process. 32 (2015) 152.

[21] M. Gancheva, I. Uzunov, R. Iordanova, K. Papazova, Mater. Chem. Phys. 164 (2015) 3645.

[22] S. Harish, J. Archana, M. Navaneethan, A. Silambarasan, K.D. Nisha, S.Ponnusamy, C. Muthamizhchelvan, H. Ikeda, D.K. Aswal, Y. Hayakawa, RSC Adv. 6 (2016) 89721.

[23] M.G. Nair, M.Nirmala,K.Rekha,A.Anukaliani, Mater.Lett. 65 (2011) 1797.

[24] H-Y. Chai , S-M. Lam, J-C. Sin, Materials Letters 242 (2019) 103.

[25] A. D. Sekar, V.Kumar, H. Muthukumar, P. Gopinath,M. Matheswaran, European Polymer Journal 118 (2019) 27.

[26] G. Vijayaprasatha, R. Murugana, S. Palanisamyb, N.M. Prabhub, T. Mahalingamc,

Y. Hayakawad, G. Ravi, Materials Research Bulletin 76 (2016) 48.

[27] H. B. Uma , S. Ananda, M.B. Nandaprakash, Chemical Data Collections 24 (2019) 100301.

[28] Z. N. Kayani, H. Bashir, S. Riaz, S. Naseem, Materials Research Bulletin 115 (2019) 121.

[29] J. Iqbal, T. Jan, M. Ismail, N. Ahmad, A. Arif, M. Khan,M. Adil, Sami-ul-Haq, A. Arshad Ceramics International40(2014)7487.

[30] M.K. Talari, A.B.A. Majeed, D.K.Tripathi, M.Tripathy,Chem. Pharm. Bull. 60 (2012)

818.

[31] O. Yamamoto, Int. J. Inorg. Mater. 3 (2001) 643.

[32] T. Nasrin, M.A. Seyedeh, D. Monir, J. Photochem. Photobiol. B:Biol. 120 (2013) 66.

[33] A. Mesaros, B. S. Vasile, D. Toloman, O.L.Pop, T. Marinca, M. Unguresan, I. Perhaita, M. Filip, F. Iordach, Appl. Surf. Sci. 471 (2019) 960.

[34] Enas N. Danial, and J.M. Yousef, J.of Pure and Appl. Microbiol., 8(1), (2014)293.

[35] K. Zhanga, Y. Zhua, X. Liua, Z. Cuib, X. Yangb, K. W.K. Yeung ,H. Pane and S. Wua,

Materials & Design 130 (2017) 403.

[36] X. Jiang, B. Zhang, B. Liua, X.Tang, L.Tang Ceramics International 45 (2019) 19948.

[37] R. K. Dutta, B. P. Nenavathu, S. Talukdar, Colloids and Surfaces B: Biointerfaces 114 (2014) 218.

[38] K. Ravichandrana, R.Rathia M.Banetoc, K.Karthikaa, P.V.Rajkumara,B. Sakthivela, R. Damodaran, Ceramics International 41(2015)3390.

[39] S. Anithaa, S. Muthukumaran, Materials Science & Engineering C 108 (2020) 110387.

[40] C. Manoharan, G. Pavithra , S. Dhanapandian, P. Dhamodharan, Spectrochimica Acta Part A: Molecular and Biomolecular Spectroscopy 149 (2015) 793.

[41] I. Ahmad, A.Z. Beg, J. Ethnopharmacol 74, (2001)113.

[42] M. Mekni, R. Azez, M. Tekaya, B. Mechri and M. Hammami J. Med. Plants Res.7(2013). 1100.

[43] R. Ebrahimifard, H. Abdizadeh and M. R. Golobostanfard, J. of Sol-Gel Science and Technology volume 93(2020)28.

[44] G.K. Williamson and H. Hall, Acta Metall. 1(1953) 22.

[45] R. Jothilakshmi,V. Ramakrishnan, R.Thangavel,J.Kumar,A.Sarua,M. Kuball,,J. Raman Spectr.40(2009)556.

[46] R. Zhang, P-G. Yin, N. Wang ,L. Guo, Solid State Sci., 11 (2009) 865.

[47] M. Yoshikawa, K. Inoue, T. Nakagawa, H. Ishida, N. Hasuike and H. Harima, Appl. Phys. Lett. 92(2008) 113115.

[48] Y. Liu, H. Zhang, X. Ann, C. Gao, Z, Zhang and J. Zhou, J. of Alloys and Compnds 506 (2010) 772.

[49] A.M. Gsiea, J.P. Goss,P.R. Briddon, R.M. Al-habashi, K.M. Etmimi, K.A.S. Marghani, WorldAcad.Sci.Eng.Technol. Int.J.Math.,Comput.,Phys.Quantum Eng.8(2014)127.

[50] K. Ravichandran, P.Ravikumar and B.Sakthivel, Appl. Surf. Sci. 287(2013)323.

[51] R. Mohan, K. Ravichandran, A.Nithya, K. Jothivenkatachalam, C. Ravidhas, B. Sakthivel, J. Mater.Sci.:Mater.Electron 25 (2014) 2546.

[52] B. Veronique, Schwartz, T. Franck, R. Sandra, P.Sabine, C. Lars, L. Alexandros, F. Renate, L. Katharina and J.Ulrich, Adv. Funct. Mater. 22(2012)2376.

[53] P. Virendra, D.Charlnene, Y.Deepti, A.J .Shaikh,V. Nadanathangam,, Spectrochim. ActaA. 65(2006)173.

[54] C.O. Tetteya, H.M. Shin,Scientific African 6(2019)157.

[55] Das D, Nath BC, Phukon P, Kalita A, Dolui SK Colloids Surf B Biointerfaces 111C(2013): 556.

[56] J. N. Schrauben, R. Hayoun, C. N. Valdez, M. Braten,L. Fridley and J. M. Mayer, Science, 336(2012)1298.

[57] A. Asok, S.Ghosh, P.A. More, B. A. Chopade, M. N. Gandhia and A. R. Kulkarni, J. Mater. Chem. B, 3 (2015) 4597.

[58] V. Murugesan, M. Saravanabhavan and M. Sekar Spectrochimica Acta Part A: Molecular and Biomolecular Spectroscopy , 147(2015)99.

[59] S. Vignesh, J. Kalyana Sundar, Applied Surface Science 449 (2018) 617.

[60] R. Karthik, S. Thambidurai, J. of Alloys and Compnds 715 (2017) 254.

[61] G. Kasi, J. Seo, Mater.Science & Engin. C 98 (2019) 717

Table I: compilation of the inhibition zone diameter against various bacteria's recorded in ZnO material doped with different metallic elements

Material	**Inhibition zone (mm)**	**Tested bacteria's**	**Ref**
Fe –ZnO	16.9	E-coli	[24]
Ni –ZnO	12 12	Streptococcus mutans P. aeruginosa	[26]
V-ZnO	19.3 12	P.aeruginosa S. Aureus	[28]
Mg-ZnO	10 10	P.aeruginosa S. Aureus	[31]
Sn –ZnO	13 10	E-Coli S. Aureus	[59]
Cu-ZnO	12 12	E-Coli S. Aureus	
Cu -Sn co-doped ZnO	16 15	E-Coli S. Aureus	
Mn- ZnO	8.8 11	E-Coli S. Aureus	[33]
Co- ZnO	8 9	E-Coli S. Aureus	[60]
Mg-ZnO	2	E-Coli	[61]
La-Cu codoped ZnO	15 14	P.aeruginosa S. Aureus	[39]
In –ZnO Thin films	12 10	Staphylococcus aureus Bacillus subtilis	[40]
Mn doped ZnO	24 22 24	E-Coli Staphylococcus aureus P.aeruginosa	[34]
In -ZnO	18 12 16 14	Bacillus subtilis S. aureus E-Coli P.aeruginosa	Present work

Figure caption

Figure 1: XRD diffraction pattern of different ZnO nanoparticles with various In doping ratios.

Figure 2: Variation of ZnO crystallite size as a function of the doping ratio.

Figure 3: Raman spectra recorded in different In doped ZnO nanoparticles.

Figure 4: SEM images of various In doped ZnO nanopowder.

Figure 5: Photoluminescence spectra recorded in different In doped ZnO nanoparticles

Figure 6: Agar plates containing zones of inhibition among the bacteria (P.aeruginosa

S. aureus and Bacillus subtilus), of ZnO where (A) ZnO pur, (B) In1ZnO (C) In3ZnO (D) In5ZnO and (E) control

Figure 7: Inhibition zone diameters against various bacteria's achieved by different In doped ZnO nanoparticles.

Figure 8: A schamatic drown illustrating the reactive oxygen species formation mechanism and the contribution of the defects Zn_i and V_{zn} as source of electrons and holes respectively.

Figure 9: : DPPH radical-scavenging activity.

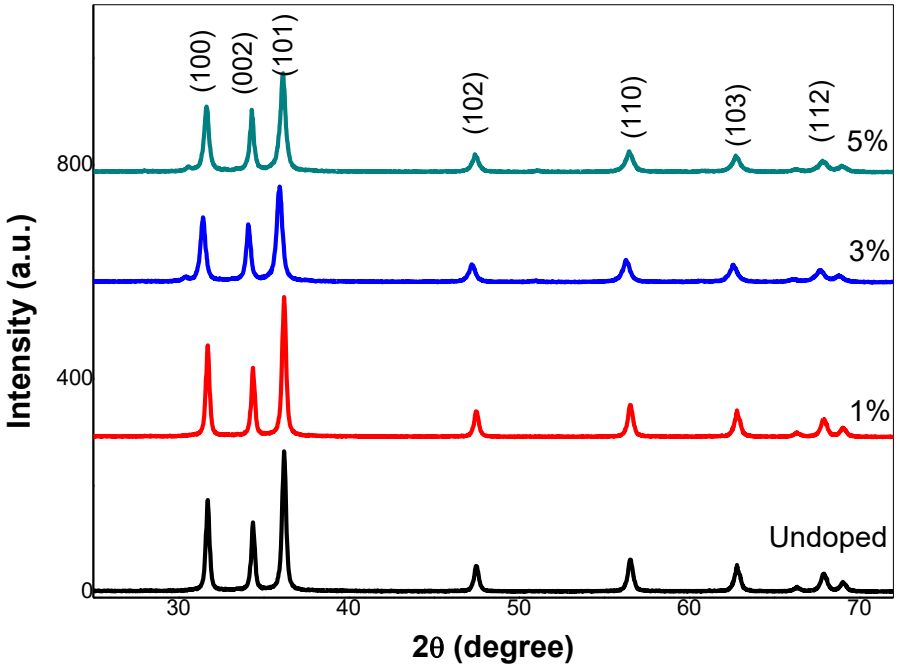

Figure 1

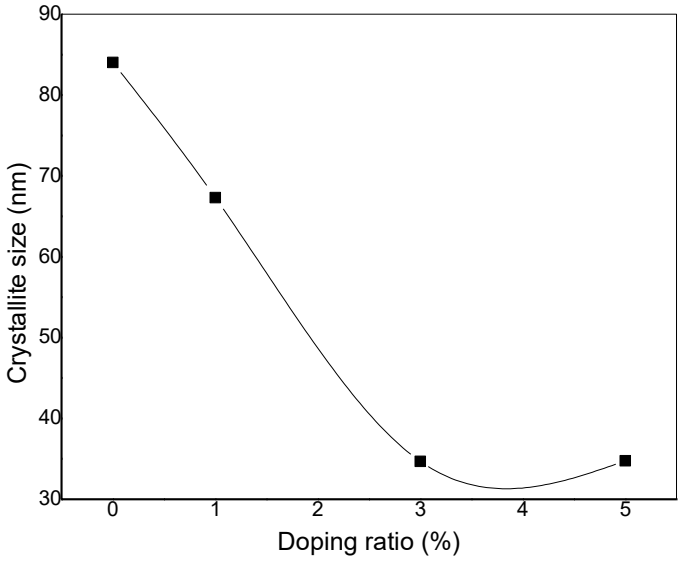

Figure 2

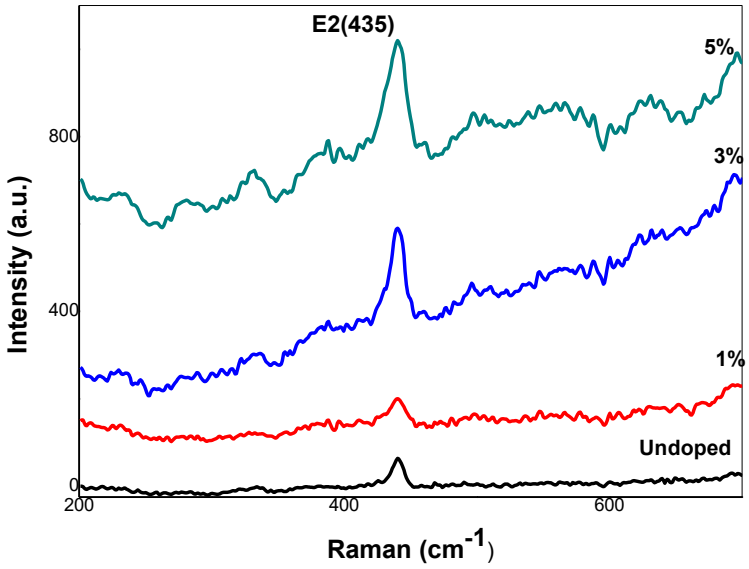

Figure 3

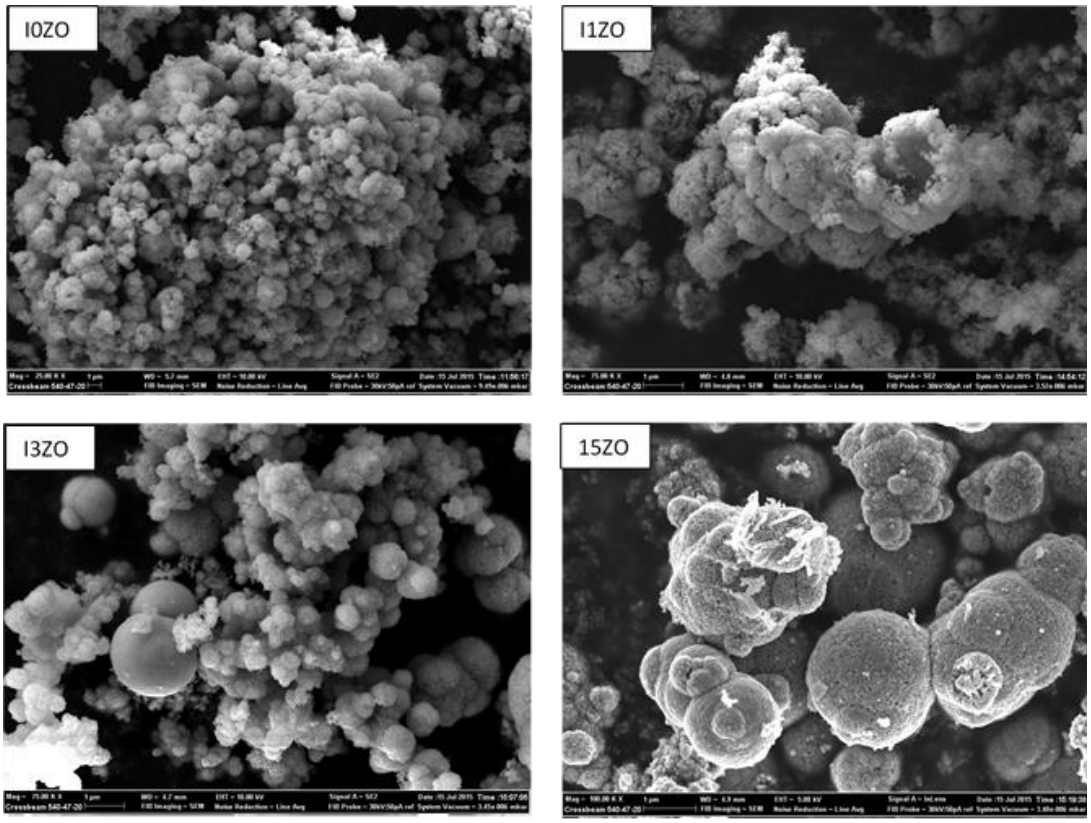

Figure 4

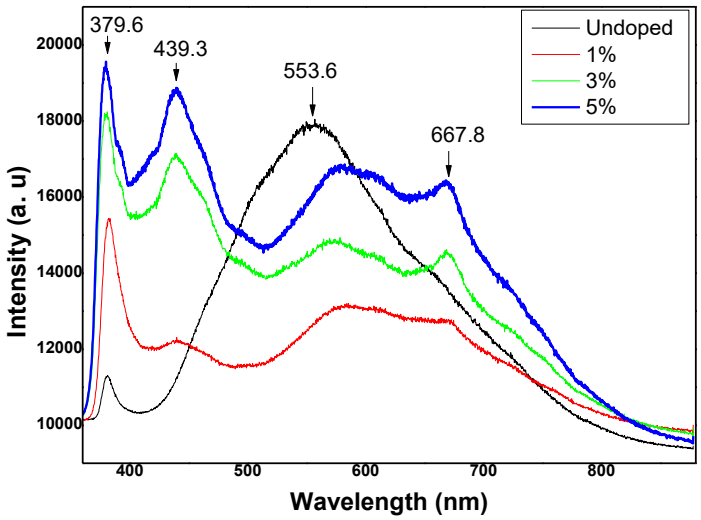

Figure 5

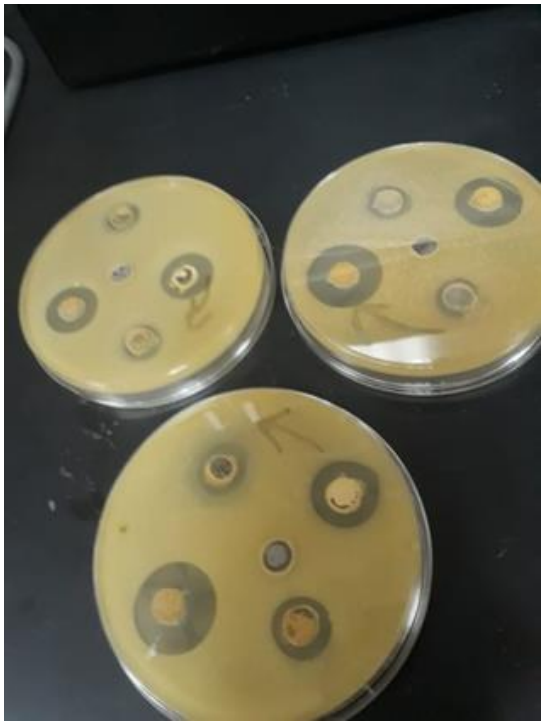

Figure 6

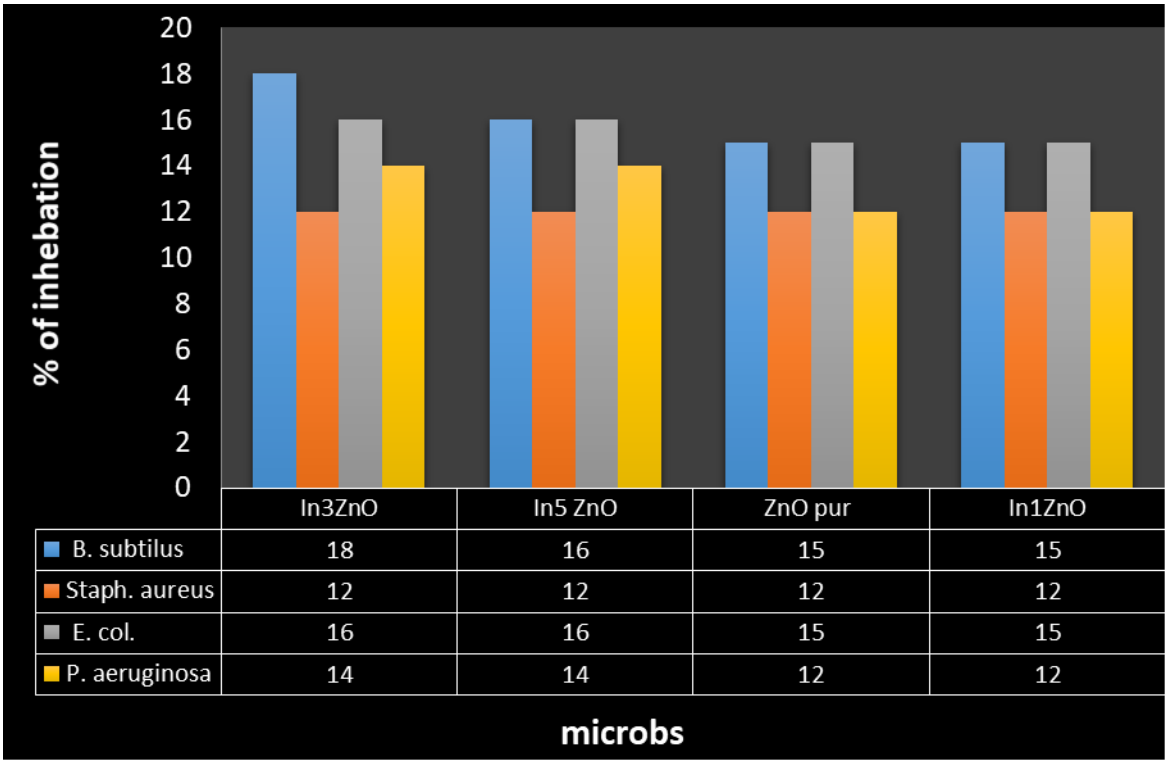

Figure 7

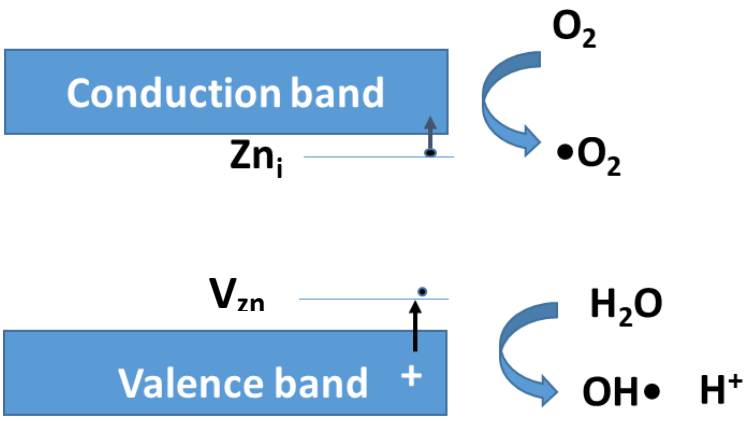

Figure 8

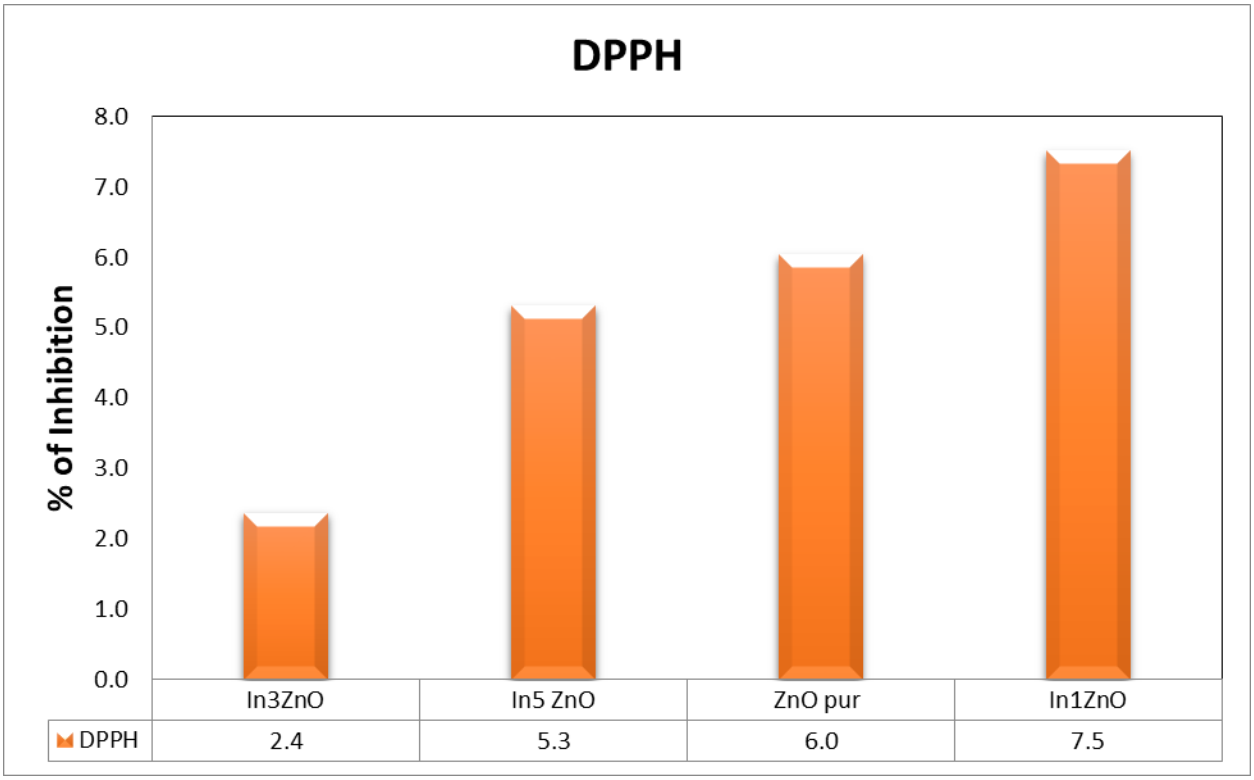
DPPH
% of Inhibition
8.0
7.0
6.0
5.0
4.0
3.0
2.0
1.0
0.0
In3ZnO
In5 ZnO
ZnO pur
In1ZnO
DPPH
2.4
5.3
6.0
7.5

Fig 9